Energy Proceedings
Vol 40, 2024
ISSN 2004-2965

A oil-water-gas three-phase flow model for flowback and early-production prediction of multi-fractured horizontal wells in lamellar shale reservoirs

Langyu Niu[1], Linsong Cheng[1], Zhikai Wang[2], Pin Jia[1]*, Yucheng Wu[1]

1 China University of Petroleum (Beijing)
(*Pin Jia: jiapin1990@163.com)

2 CNOOC Research Institute Ltd.

ABSTRACT

Some of the beddings in lamellar shale oil reservoir are opened and intersected with the hydraulic fractures, result in orthogonal fracture networks, after hydraulic fracturing. Which make it difficult to interpret properties of fractured reservoir, and affecting the accuracy of production prediction. In this work, a new semi-analytical model is developed specifically for modeling oil-water-gas three-phase production during flowback and early-time production for lamellar shale oil reservoirs. Two flow regions are assumed: opened beddings and matrix, which is considered as dual-medium model, including shale matrix and unopened beddings. A semi-analytical solution method based on dynamic drainage area (DDA) concept is used to solve the mathematical model, in order to improve the accuracy of initial time steps. Stress-dependent and saturation-dependent properties of fractures and matrix are handled in the solution. The robustness of the innovative model is tested through comparison with rigorous numerical model. Based on the proposed model, the influencing factors of three-phase flowback performance for multi-fractured horizontal wells in lamellar shale oil reservoir are clarified. The model in this study provides a foundation for efficient automatic history matching.

Keywords: shale oil reservoir, multi-phase flowback and early production, mathematical model

NONMENCLATURE

Abbreviations	
DDA	Dynamic Drainage Area
MFHW	Multi-Fractured Horizontal Well
DOI	Dynamic Of Investigation
BPP	Bubble Point Pressure
MBE	Material Balance Equation
Symbols	
d	Days
k	Permeability
ϕ	Porosity
S	Saturation
B	Volume factor
R_s	Gas oil ratio
k_r	Relative permeability
T	Productivity index
μ	Viscosity
c	Compressibility
N	Total production till last time step
β	Unit conversion factor

1. INTRODUCTION

Shale reservoirs have gradually become an important source of hydrocarbon due to dwindling supply of hydrocarbon from conventional coupled with rapidly increasing energy demands[1-3]. As a potential conventional energy resource, shale oil has attracted much attention[4,5]. As a typical unconventional reservoir, shale reservoir is composed of matrix and beddings[6-8], which characteristics affect fluids flow in shale reservoir. Forecasts of oil, water and gas production for shale oil wells are important in economic valuation of these un conventional plays[9].

Compared with the numerical simulation semi-analytical models and analytical models are computationally cheaper, but compromise some of the important physics of the problem especially in the flow of shale matrix[10]. Clarkson and Williams-Kovacs proposed a conceptual model DDA, which has been revised to increase flexibility for inclusion of additional physics in shale matrix, this method has been applied in

This is a paper for 15th International Conference on Applied Energy (ICAE2023), Dec. 3-7, 2023, Doha, Qatar.

tight reservoir (multi-fractured horizontal wells)MFHWs' history matching[11].

In lamellar shale oil reservoirs, the fracture-bearing shale has a complex rock mass with layered structure, which makes the construction conditions of reservoir reconstruction more complicated and construction more complex[12-14]. As demonstrated in the laboratory fracturing simulation and field fracture monitoring, bedding fractures have an important impact on the vertical extension and propagation morphology of hydraulic fractures[15,16]. After hydraulic fracturing, under small in-situ stress difference, high pressure fracturing fluids are injected, some beddings opened and intersected with the hydraulic fractures, result in orthogonal fracture networks[17].

In this study, a mathematical model for oil, gas, and water three-phase flowback and early-production is established, in which consider opened beddings, and matrix, the hydraulic fracture is regarded as infinite conductivity. In order to improve the accuracy of initial time steps DDA concept is introduced for solving the mathematical model semi-analytically. The accuracy of proposed model is demonstrated through comparison to numerical simulation. And it shows much computationally cheaper. The main influencing factors of flowback and early production have been clarified.

2. METHODOLOGY

2.1 Physical model

In lamellar shale reservoirs, beddings are usually extremely developed. After hydraulic fracturing, the hydraulic fracture is easy to turn along the direction of the beddings, forming orthogonal fracture networks in the vertical direction, especially when the reservoir rock is brittle and the in-situ stress difference is small. At the same time, during the hydraulic fracturing process, high-pressure fracturing fluid opened some of beddings and drove the oil phase away from the fractures, which result in a high-pressure and high-water saturation region in the fracture system. Fig. 1 shows a triple medium physical model. In this physical model, the reservoir after hydraulic fracturing is divided into hydraulic fracture, opened beddings, and matrix (this area actually includes shale matrix and unopened beddings, and the physical parameters of this area are represented by the equivalent parameters by Kazemi dual-media model). The interference between the joints fractures is considered by considering the closed boundary between the opened beddings.

For the physical model in this chapter, the following assumptions are made:

(1) The reservoir is of equal thickness and ignores the influence of gravity, with hydraulic fractures penetrating the reservoir vertically;

(2) The water saturation in opened bedding is 1;

(3) The pressure inside opened beddings is much higher than the original formation pressure, approaching the reservoir fracture pressure;

(4) The fluid flows from the matrix into the opened beddings, and then into the hydraulic fractures through the opened beddings;

(5) During the flowback process, opened beddings is affected by stress sensitivity;

(6) Hydraulic fractures are considered as infinite conductivity.

2.2 Mathematical model

Multi-phase fluids flow in each region can be regarded as linear flow, under this assumption, the mathematical model can be expressed as follows.

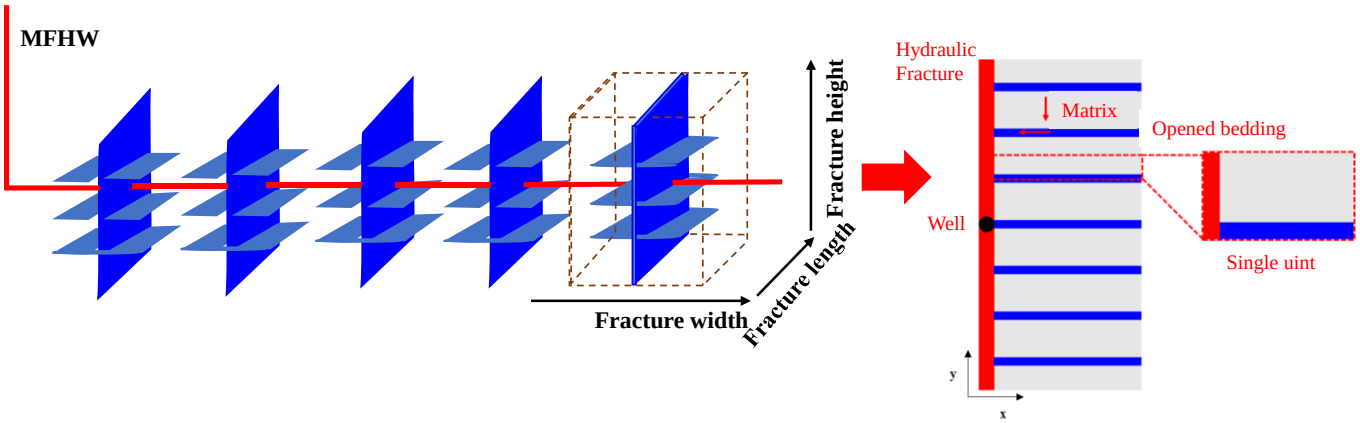

Fig. 1 Physical model diagram

2.2.1 Matrix flow equations

water phase:

$$\frac{\partial}{\partial y}\left(\frac{\beta k_{\mathrm{m}} k_{\mathrm{rwm}}}{\mu_{\mathrm{wm}} B_{\mathrm{wm}}} \frac{\partial p_{\mathrm{m}}}{\partial y}\right)=\frac{\partial}{\partial t}\left(\frac{\phi_{\mathrm{m}} S_{\mathrm{wm}}}{B_{\mathrm{wm}}}\right) \tag{1}$$

Gas phase(above BBP):

$$\frac{\partial}{\partial y}\left(\frac{\beta k_{\mathrm{m}} k_{\mathrm{rgm}}}{\mu_{\mathrm{gm}} B_{\mathrm{gm}}} \frac{\partial p_{\mathrm{m}}}{\partial y}\right)=\frac{\partial}{\partial t}\left(\frac{\phi_{\mathrm{m}} S_{\mathrm{gm}}}{B_{\mathrm{gm}}}\right) \tag{2}$$

Gas phase(below BBP):

$$\frac{\partial}{\partial y}\left[\left(\frac{R_{\mathrm{s}} \beta k_{m} k_{\mathrm{rom}}}{\mu_{\mathrm{om}} B_{\mathrm{om}}}+\frac{\beta k_{\mathrm{m}} k_{\mathrm{rgm}}}{\mu_{\mathrm{gm}} B_{\mathrm{gm}}}\right) \frac{\partial p_{\mathrm{m}}}{\partial y}\right]=\frac{\partial}{\partial t}\left(\frac{R_{\mathrm{s}} \phi_{\mathrm{m}} S_{\mathrm{om}}}{B_{\mathrm{om}}}+\frac{\phi_{\mathrm{m}} S_{\mathrm{gm}}}{B_{\mathrm{gm}}}\right) \tag{3}$$

Oil phase:

$$\frac{\partial}{\partial y}\left(\frac{\beta k_{m} k_{\mathrm{rom}}}{\mu_{\mathrm{om}} B_{\mathrm{om}}} \frac{\partial p_{m}}{\partial y}\right)=\frac{\partial}{\partial t}\left(\frac{\phi_{m} s_{\mathrm{om}}}{B_{\mathrm{om}}}\right) \tag{4}$$

In the subscript, "m" represents the matrix, "n" represents the opened bedding fracture, "w" represents water phase, "o" represents oil phase, "g" represents gas phase, "o-g" represents dissolved gas. If the equation is the same for three-phase, the subscript is "j"In the formula, β is the unit conversion coefficient, which is 0.0864 under the international system of units; k_{m} is the matrix permeability, mD; k_{rwm} is the water phase relative permeability in the matrix, dimensionless; p_{m} is the average pressure within the matrix, MPa; μ_{wm} is the water phase viscosity within the matrix. mPa·s； B_{wm} is the volume factor of the water phase in the matrix, dimensionless; φ_{m} is the porosity of the matrix, dimensionless; S_{wm} is the average water saturation within the matrix, dimensionless; R_{s} represents the dissolved gas oil ratio, m^3/m^3, defined as the ratio of the volume of the oil phase to the volume of the gas phase under standard conditions.

The initial conditions are:

$$p_{\mathrm{m},t=0}=p_{\mathrm{i}} \tag{5}$$

Assuming a closed outer boundary condition:

$$\left.\frac{\partial p_{\mathrm{m}}}{\partial y}\right|_{y=y_{\mathrm{out}}}=0 \tag{6}$$

The matrix is coupled with the opened bedding fractures through the material balance method. Material balance is different, when the pressure is above or below the bubble point pressure (BPP):

Above BPP:

$$q_{\mathrm{mj,\ flow\text{-}in}}=q_{\mathrm{mj,\ flow\text{-}out}} \tag{7}$$

Below BPP:

$$q_{\mathrm{mg,flow-in}}+q_{\mathrm{mo\text{-}g,flow-in}}=q_{\mathrm{mg,flow-out}}+q_{\mathrm{mo\text{-}g,flow-out}} \tag{8}$$

2.2.2 Opened beddings flow equation

Water phase:

$$\frac{\partial}{\partial x}\left(\frac{\beta k_{n} k_{\mathrm{rwn}}}{\mu_{\mathrm{wn}} B_{\mathrm{wn}}} \frac{\partial p_{n}}{\partial x}\right)+q_{\mathrm{wm}}=\frac{\partial}{\partial t}\left(\frac{\phi_{n} S_{\mathrm{wn}}}{B_{\mathrm{wn}}}\right) \tag{9}$$

Gas phase(above BBP):

$$\frac{\partial}{\partial x}\left(\frac{\beta k_{n} k_{\mathrm{rgn}}}{\mu_{gn} B_{gn}} \frac{\partial p_{n}}{\partial x}\right)+q_{\mathrm{gm}}=\frac{\partial}{\partial t}\left(\frac{\phi_{n} S_{gn}}{B_{gn}}\right) \tag{10}$$

Gas phase(below BBP):

$$\frac{\partial}{\partial x}\left[\left(\frac{R_{\mathrm{S}} \beta k_{\mathrm{n}} k_{\mathrm{ron}}}{\mu_{\mathrm{on}} B_{\mathrm{on}}}+\frac{\beta k_{\mathrm{n}} k_{\mathrm{rgn}}}{\mu_{\mathrm{gn}} B_{\mathrm{gn}}}\right) \frac{\partial p_{\mathrm{n}}}{\partial x}\right]+q_{\mathrm{gm}}=\frac{\partial}{\partial t}\left(\frac{R_{\mathrm{S}} \phi_{\mathrm{n}} S_{\mathrm{on}}}{B_{\mathrm{on}}}+\frac{\phi_{\mathrm{n}} S_{\mathrm{gn}}}{B_{\mathrm{gn}}}\right) \tag{11}$$

Oil phase:

$$\frac{\partial}{\partial x}\left(\frac{\beta k_{n} k_{\mathrm{ron}}}{\mu_{\mathrm{on}} B_{\mathrm{on}}} \frac{\partial p_{n}}{\partial x}\right)+q_{\mathrm{om}}=\frac{\partial}{\partial t}\left(\frac{\phi_{n} S_{\mathrm{on}}}{B_{\mathrm{on}}}\right) \tag{12}$$

The initial conditions is:

$$p_{\mathrm{n},t=0}=p_{\mathrm{break}} \tag{13}$$

Assuming infinite conductivity in the wellbore and hydraulic fractures, the internal boundary conditions for opening beddings is:

$$p_{\mathrm{n}}\big|_{x=\mathrm{f}}=p_{\mathrm{wf}} \tag{14}$$

2.3 Semi-analytical solution

The flow rate from matrix to opened beddings, and from beddings to hydraulic fracture can be expressed as productivity index and pressure difference. The productivity index has been proposed by Wattenbarger[18] in 1998.

Fig.2 shows multi-phase fluids flow from matrix to opened beddings.

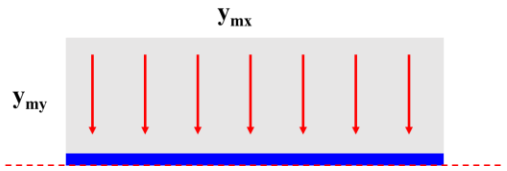

Fig. 2 Fluids flow from shale matrix to opened beddings

Productivity index of fluids flow from matrix to opened beddings can be expressed as:

Oil, water and gas:

$$T_{\mathrm{jm\text{-}n}}=\frac{k_{m} k_{\mathrm{rjm}} h}{1.842 B_{\mathrm{jm}} \mu_{\mathrm{jm}}\left[\frac{2}{\pi}\left(\frac{y_{\mathrm{my}}}{y_{\mathrm{mx}}}\right)\right]} \tag{15}$$

Dissolved gas：

$$T_{\mathrm{ogm\text{-}n}}=\frac{R_{s} k_{m} k_{\mathrm{rom}} h}{1.842 B_{\mathrm{om}} \mu_{\mathrm{om}}\left[\frac{2}{\pi}\left(\frac{y_{\mathrm{my}}}{y_{\mathrm{mx}}}\right)\right]} \tag{16}$$

Fig.3 shows multi-phase fluids flow from opened beddings to hydraulic fracture.

Oil, water and gas:

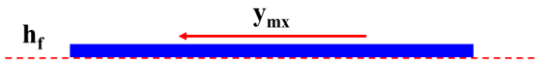

Fig. 3 Fluids flow from opened bedding to hydraulic fracture

$$T_{\mathrm{jn-f}}=\frac{k_{\mathrm{n}}k_{\mathrm{rjn}}h}{1.842B_{\mathrm{jn}}\mu_{\mathrm{jn}}\left[\frac{2}{\pi}\left(\frac{y_{\mathrm{mx}}}{w_{\mathrm{n}}}\right)\right]} \tag{17}$$

Dissolved gas：

$$T_{\mathrm{ogn-f}}=\frac{R_s k_n k_{\mathrm{ron}}h}{1.842B_{\mathrm{on}}\mu_{\mathrm{on}}\left[\frac{2}{\pi}\left(\frac{y_{\mathrm{mx}}}{w_n}\right)\right]} \tag{18}$$

Fluids flow is characterized by average pressure and saturation in pseudo steady-state flow. However, due to the ultra-low permeability of shale matrix, using average pressure and saturation cannot accurately describe the flow of fluid within the matrix. Therefore, DDA is introduced to improve the calculation accuracy of the initial time step.

Combine the matrix control equations of oil gas water three-phase flow and establish a control equation for oil gas water three-phase flow[19]:

$$\frac{\partial}{\partial x}\left[\beta\rho_{\mathrm{wstd}}\frac{k_m k_{\mathrm{rwm}}}{\mu_{wm}B_{wm}}\frac{\partial p_m}{\partial x}\right]+\frac{\partial}{\partial x}\left[\beta\rho_{\mathrm{ostd}}\frac{k_m k_{\mathrm{rom}}}{\mu_{\mathrm{om}}B_{\mathrm{om}}}\frac{\partial p_m}{\partial x}\right]+\frac{\partial}{\partial x}\left[\beta\rho_{\mathrm{gstd}}k_m\left(\frac{R_s k_{\mathrm{rom}}}{\mu_{\mathrm{om}}B_{\mathrm{om}}}+\frac{k_{\mathrm{rgm}}}{\mu_{gm}B_{gm}}\right)\frac{k_{\mathrm{rgm}}}{\mu_{gm}B_{gm}}\frac{\partial p_m}{\partial x}\right]$$
$$=\frac{\partial}{\partial t}\left(\frac{\rho_{\mathrm{wstd}}\phi_m S_{\mathrm{wm}}}{B_{\mathrm{wm}}}\right)+\frac{\partial}{\partial t}\left(\frac{\rho_{\mathrm{ostd}}\phi_m S_{\mathrm{om}}}{B_{\mathrm{om}}}\right)+\frac{\partial}{\partial t}\left(\frac{\rho_{\mathrm{gstd}}\phi_m S_{gm}}{B_{gm}}+\frac{R_s\phi_m\rho_{\mathrm{ostd}}S_{\mathrm{om}}}{B_{\mathrm{om}}}\right) \tag{19}$$

The dynamic of investigation (DOI) of matrix can be expressed in formula (20), both y_{mx} and y_{my} can be calculate by this formula.

$$y_{\mathrm{m}}=\sqrt{6\eta t} \tag{20}$$

Where η It can be expressed as:

$$\eta=\frac{a_{lw}+a_{\mathrm{lo}}+a_{\mathrm{lg}}}{a_{\mathrm{rw}}+a_{\mathrm{ro}}+a_{\mathrm{rg}}} \tag{21}$$

Among them:

$$a_{\mathrm{lw}}=\frac{\beta\rho_{\mathrm{wstd}}k_m k_{\mathrm{rwm}}}{\mu_{wm}B_{wm}},a_{\mathrm{lg}}=\beta\rho_{\mathrm{gstd}}k_m\left(\frac{R_s k_{\mathrm{rom}}}{\mu_{\mathrm{om}}B_{\mathrm{om}}}+\frac{k_{\mathrm{rgm}}}{\mu_{gm}B_{gm}}\right),a_{lo}=\frac{\beta\rho_{\mathrm{ostd}}k_m k_{\mathrm{rom}}}{\mu_{\mathrm{om}}B_{\mathrm{om}}}$$
$$a_{\mathrm{rw}}=\frac{(c_m+c_w)\phi_m\rho_{\mathrm{wstd}}S_{wm}}{B_{wm}},a_{\mathrm{ro}}=\frac{(c_m+c_o)\phi_m\rho_{\mathrm{ostd}}S_{\mathrm{om}}}{o},a_{\mathrm{rg}}=\frac{(c_m+c_g)\phi_m\rho_{\mathrm{gstd}}S_{gm}}{B_{gm}}+\frac{(c_m+c_o)\phi_m R_s\rho_{\mathrm{ostd}}S_{\mathrm{om}}}{B_{\mathrm{om}}} \tag{21}$$

In the formula, c_{m} is the compression coefficient of shale matrix, MPa^{-1}. c_{w} 、 c_{o} 、 c_{g} is the compressibility coefficients of water phase, oil phase, and gas phase, MPa^{-1}, respectively.

After calculate the flow rate of each phase and each region, material balance method is used to calculate the average pressure and average saturation. Due to the involvement of oil, gas, and water three-phase flow, the material balance equations (MBEs) needs to consider two situations: fluid pressure higher than BPP and fluid pressure lower than BPP. When the fluid pressure is higher than the BPP, the flow in this region of the reservoir is three-phase flow, with no gas phase separating from the oil phase. When the fluid pressure is lower than the BPP, dissolved gas escape from the oil phase, so it is necessary to add a material balance equation for the dissolved gas phase. MBEs of matrix can be expressed as follows.

Water phase:

$$4y_{\mathrm{mx}}hy_{\mathrm{my}}\left(\frac{\phi_{\mathrm{mi}}S_{\mathrm{wmi}}}{B_{\mathrm{wmi}}}-\frac{\phi_{\mathrm{m}}S_{\mathrm{wm}}}{B_{\mathrm{wm}}}\right)=\left[N_{\mathrm{wm\text{-}n}}+T_{\mathrm{wm\text{-}n}}\left(p_{\mathrm{m}}-p_{\mathrm{n}}\right)\Delta t\right] \tag{23}$$

Oil phase:

$$4y_{\mathrm{mx}}hy_{\mathrm{my}}\left(\frac{\phi_{\mathrm{mi}}S_{\mathrm{omi}}}{B_{\mathrm{omi}}}-\frac{\phi_{\mathrm{m}}S_{\mathrm{om}}}{B_{\mathrm{om}}}\right)=\left[N_{\mathrm{om\text{-}n}}+T_{\mathrm{om\text{-}n}}\left(p_{\mathrm{m}}-p_{\mathrm{n}}\right)\Delta t\right] \tag{24}$$

Gas phase：

$$4y_{\mathrm{mx}}hy_{\mathrm{my}}\left(\frac{\phi_{\mathrm{mi}}S_{\mathrm{gmi}}}{B_{\mathrm{gmi}}}-\frac{\phi_{\mathrm{m}}S_{\mathrm{gm}}}{B_{\mathrm{gm}}}\right)=\left[N_{\mathrm{gm\text{-}n}}+T_{\mathrm{gm\text{-}n}}\left(p_{\mathrm{m}}-p_{\mathrm{n}}\right)\Delta t\right] \tag{25}$$

The gas phase material balance equation below the bubble point pressure can be expressed as:

$$4y_{\mathrm{mx}}hy_{\mathrm{my}}\left(\frac{\phi_{\mathrm{mi}}S_{\mathrm{gmi}}}{B_{\mathrm{gmi}}}-\frac{\phi_{\mathrm{m}}S_{\mathrm{gm}}}{B_{\mathrm{gm}}}\right)+4y_{\mathrm{mx}}hy_{\mathrm{my}}\left(\frac{R_{\mathrm{smi}}\phi_{\mathrm{mi}}S_{\mathrm{omi}}}{B_{\mathrm{omi}}}-\frac{R_{\mathrm{sm}}\phi_{\mathrm{m}}S_{\mathrm{om}}}{B_{\mathrm{om}}}\right)$$
$$=\left[N_{\mathrm{gm\text{-}n}}+T_{\mathrm{gm\text{-}n}}\left(p_m-p_n\right)\Delta t\right]+\left[N_{\mathrm{ogm\text{-}n}}+T_{\mathrm{ogm\text{-}n}}\left(p_m-p_n\right)\Delta t\right] \tag{26}$$

R_{smi} is the dissolved gas oil ratio under initial conditions, m^3/m^3; R_{sm} is the dissolved gas oil ratio at the current time step, m^3/m^3. Referring to the material balance equation in the shale matrix region, when the fluid pressure is higher than the BPP, the material balance equation in the opened bedding can be expressed as:

Oil phase:

$$4y_{\mathrm{mx}}hw_{\mathrm{n}}\left(\frac{\phi_{\mathrm{ni}}S_{\mathrm{oni}}}{B_{\mathrm{oni}}}-\frac{\phi_{n}S_{\mathrm{on}}}{B_{\mathrm{on}}}\right)=\left[N_{\mathrm{on\text{-}f}}+T_{\mathrm{on\text{-}f}}\left(p_{\mathrm{n}}-p_{\mathrm{f}}\right)\Delta t\right]-\left[N_{\mathrm{om\text{-}n}}+T_{\mathrm{om\text{-}n}}\left(p_{\mathrm{m}}-p_{\mathrm{n}}\right)\Delta t\right] \tag{27}$$

Water phase:

$$4y_{\mathrm{mx}}hw_{\mathrm{n}}\left(\frac{\phi_{\mathrm{ni}}S_{\mathrm{wni}}}{B_{\mathrm{wni}}}-\frac{\phi_{n}S_{\mathrm{wn}}}{B_{\mathrm{wn}}}\right)=\left[N_{\mathrm{wn\text{-}f}}+T_{\mathrm{wn\text{-}f}}\left(p_{\mathrm{n}}-p_{\mathrm{f}}\right)\Delta t\right]-\left[N_{\mathrm{wm\text{-}n}}+T_{\mathrm{wm\text{-}n}}\left(p_{\mathrm{m}}-p_{\mathrm{n}}\right)\Delta t\right] \tag{28}$$

Gas phase:

$$4y_{\mathrm{mx}}hw_{\mathrm{n}}\left(\frac{\phi_{\mathrm{ni}}S_{\mathrm{gni}}}{B_{\mathrm{gni}}}-\frac{\phi_{n}S_{\mathrm{gn}}}{B_{\mathrm{gn}}}\right)=\left[N_{\mathrm{gn\text{-}f}}+T_{\mathrm{gn\text{-}f}}\left(p_{\mathrm{n}}-p_{\mathrm{f}}\right)\Delta t\right]-\left[N_{\mathrm{gm\text{-}n}}+T_{\mathrm{gm\text{-}n}}\left(p_{\mathrm{m}}-p_{\mathrm{n}}\right)\Delta t\right] \tag{29}$$

When the fluid pressure is lower than BPP, MBE of gas phase can be expressed as:

$$4y_{\mathrm{mx}}hv_{\mathrm{n}}\left(\frac{\phi_{\mathrm{ni}}S_{\mathrm{gni}}}{B_{\mathrm{gni}}}-\frac{\phi_{n}S_{\mathrm{gn}}}{B_{\mathrm{gn}}}\right)+4y_{\mathrm{mx}}hw_{\mathrm{n}}\left(\frac{R_{\mathrm{sni}}\phi_{\mathrm{ni}}S_{\mathrm{oni}}}{B_{\mathrm{oni}}}-\frac{R_{sn}\phi_{\mathrm{n}}S_{\mathrm{on}}}{B_{on}}\right)$$
$$=\left[N_{\mathrm{gn-f}}+T_{\mathrm{gn-f}}\left(p_{\mathrm{n}}-p_{\mathrm{f}}\right)\Delta t\right]-\left[N_{\mathrm{gm\text{-}n}}+T_{\mathrm{gm\text{-}n}}\left(p_{\mathrm{m}}-p_{\mathrm{n}}\right)\Delta t\right]$$
$$+\left[N_{\mathrm{ogn\text{-}f}}+T_{\mathrm{ogn-f}}\left(p_{\mathrm{n}}-p_{\mathrm{f}}\right)\Delta t\right]-\left[N_{\mathrm{ogm\text{-}n}}+T_{\mathrm{ogm\text{-}n}}\left(p_{\mathrm{m}}-p_{\mathrm{n}}\right)\Delta t\right] \tag{30}$$

The permeability and porosity of each region are consider stress sensitive, and adopt exponential formulas. The specific solution process is shown in Fig. 4.

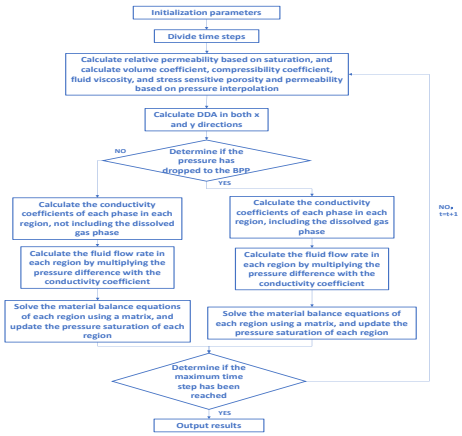

Fig. 4 Calculation flowchart

2.4 Model verification

Compare the calculation results of proposed model with the commercial numerical simulation software tNavigator for model verification, and evaluate the accuracy and applicability of the established model. The scheme and griding of the numerical model is shown in Fig.5.

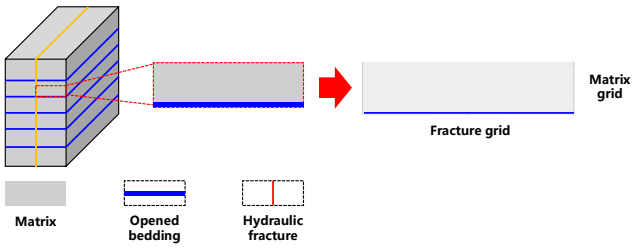

Fig. 5 Schematic diagram and meshing of numerical model

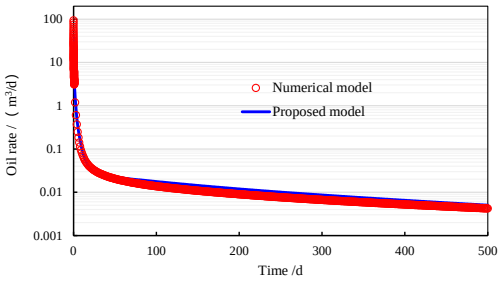

(a) Oil rate

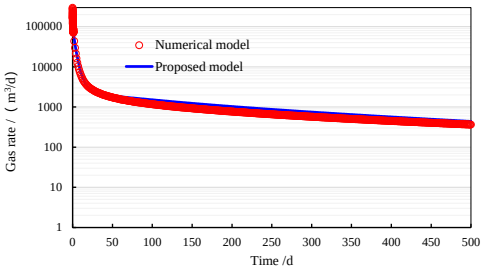

(b) Gas rate

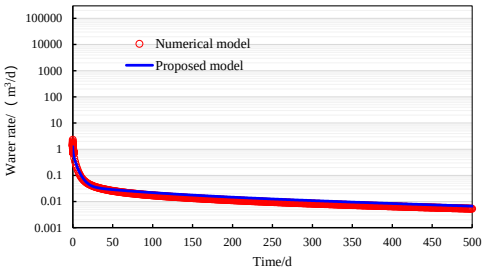

(c) Water rate

Fig. 6 Verification result

It can be seen that proposed model matches well with commercial numerical simulation software. The accuracy of proposed model is confirmed.

3. DISCUSSION

After establishing a semi-analytical model for oil-water-gas three-phase flowback in shale reservoir. In this section, we discussed factors which affect flowback and production performance based on proposed model.

3.1 Permeability of opened bedding

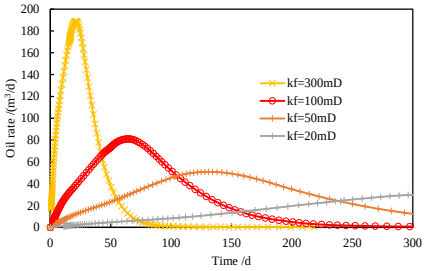

(a) Oil rate

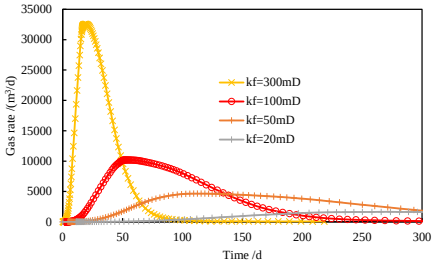

(b)Gas rate

Fig. 7 Influence of opened bedding's permeability

As shown in Fig.7, with the increase in the permeability of the opened bedding, the peak of oil rate appears earlier, and the decline rate of oil rate after reaching the peak also increases. Gas rate is greatly affected by the permeability of the opened bedding. Similar to the variation pattern of oil phase, as the permeability of the opened bedding increases, gas rate curve reaches the peak earlier, and the decrease after reaching the peak becomes faster.

3.2 Matrix permeability

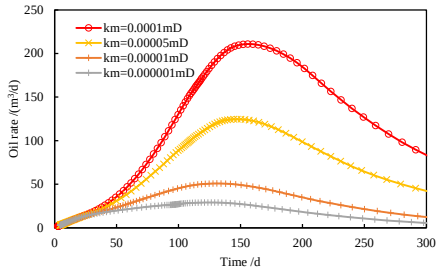

(a) Oil rate

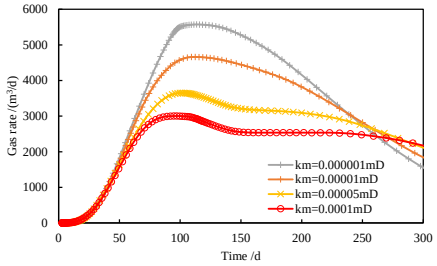

(b)Gas rate

Fig. 8 Influence of matrix permeability

As shown in Fig. 8, when the matrix permeability is high, there is a clear turning point at the peak of the oil rate curve. When the matrix permeability is low, the peak of the oil rate curve is not obvious, indicating that the matrix supply capacity is weak. After the oil rate reaches its peak, its decline rate increases with the increase of matrix permeability. The matrix permeability has almost no effect on the time when oil rate reaches its peak. With the increasing of matrix permeability, gas rate significantly decreases. This is because the increase of matrix permeability leads to a decrease in the pressure difference between the matrix and the opened bedding, which slows down the rate of pressure drop inside the opened bedding, and reduces the amount of gas escape from the oil phase. The time when gas rate reaches its peak is almost unaffected by matrix permeability. The four sets of data in the figure almost reach the peak at the same time.

3.3 Average pore size of matrix

The average pore size of the matrix will affect the PVT parameters of the reservoir fluid, mainly reflected in the value of bubble point pressure and the distribution of dissolved gas oil ratio in this model. Fig. 9 is the oil-gas phase diagram, the envelope curve become smaller with the decreasing of pore size[20].

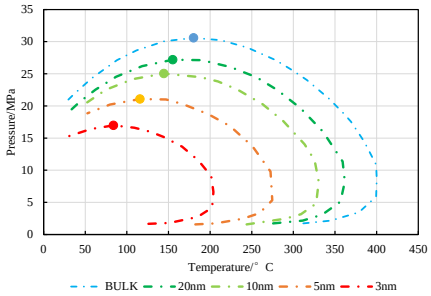

Fig. 9 Phase diagram under different pore size

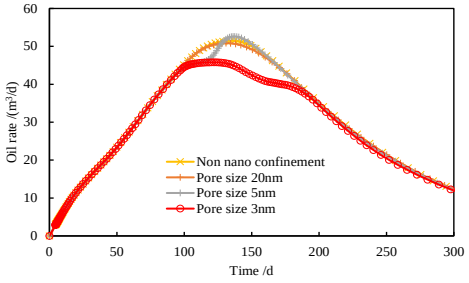

(a) Oil rate

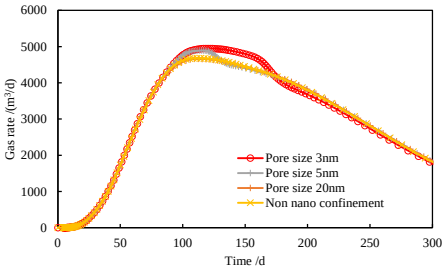

(b)Gas rate

Fig. 10 Influence of Average pore size of matrix

As shown in Fig. 10(a), as the average pore size of the matrix decreases, the peak of oil rate significantly decreases under the same conditions. The micropores in shale matrix can reach below 3nm, so its impact on oil phase flow-back performance cannot be ignored. As shown in Fig. 10(b), the peak production of the gas rate significantly increases with the decrease of the average pore size of the matrix. As the average pore size of the shale matrix decreases, gas rate increases and the peak of it is delayed.

3.4 Flowback strategy

As shown in Fig. 11, assuming the BPP to 25MPa, and set three different backflow strategies. The first type is

pressure control backflow, which controls the bottom hole pressure to be higher than the BPP. The second type is blowout backflow, where the bottomhole pressure continues to decrease and there is no significant slope change in the flow pressure curve. The third type is fast blowout flowback, where the bottom hole flow pressure rapidly decreases and slowly decreases after reaching the equivalent liquid column pressure of the reservoir.

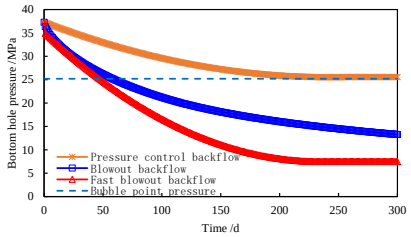

Fig. 11 Bottom hole pressure of three flowback strategy

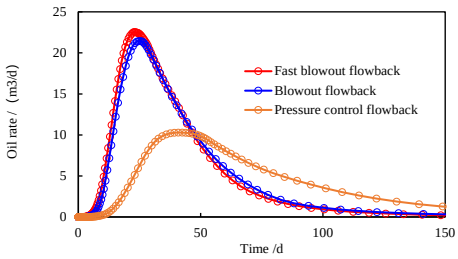

(a) Oil rate

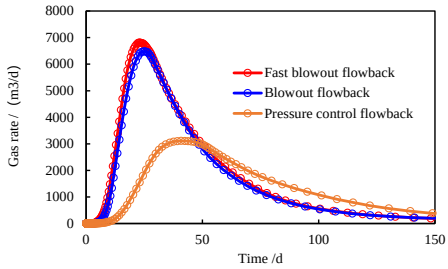

(b)Gas rate

Fig. 12 Influence of flowback strategy

As shown in Fig. 12, with the increasing of the initial decrease rate of bottom hole pressure, the peak of oil and gas rate becomes higher and earlier. Affected by the release of dissolved gas and stress sensitivity, the oil rate of pressure control flowback after reaching the peak is higher than that of fast blowout flowback and blowout flowback. The same curve pattern appears in gas rate curves. Therefore, in the backflow process of shale oil reservoir, the size of the oil nozzle should be controlled to reduce the severe stress sensitivity and dissolved gas release effect caused by excessive pressure drop.

4. APPLICATION

The Daqing Gulong shale oil reservoir belongs to the lamellar shale reservoir. Due to the small horizontal stress difference and extremely developed beddings fractures in this block, core experiments have shown that hydraulic fractures are difficult to develop along the perforation direction, and are easy to turning along the bedding fracture direction, forming orthogonal fracture networks, which is similar to the physical model assumption in this paper. We combine proposed model with genetic algorithm (GA), matching the calculate production with the flowback datum automatically. Through which, the key parameters of fractures network can be interpreted.

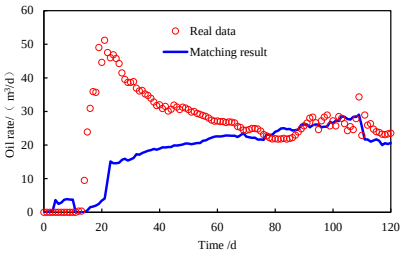

(a) Oil rate

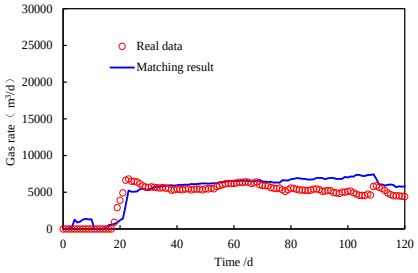

(b)Gas rate

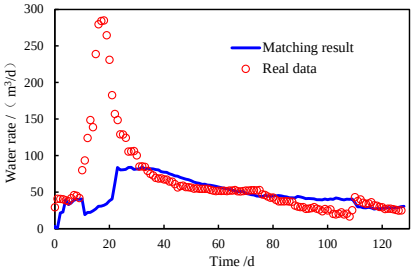

(c)Water rate

Fig. 13 Automatic history matching result

The matching results are shown in Fig. 13, the initial matching effect is poor, which is because the proposed model has ignored long distance horizontal well and hydraulic fracture. As the result, matching result is much lower than the real flowback datum. The key parameters of shale matrix and fracture network can be interpreted through history matching. The half length of Single cluster is 46.32m, the number of opened in one meter is 0.36, the half length of opened beddings 5.62m, the

permeability of opened bedding is 12.76 mD, the permeability of shale matrix is 7.44×10^{-4}mD.

5. CONCLUSIONS

The primary contribution of the paper is the provision of an approximate mathematic model with semi-analytical solution, which can predict the flowback and early-production performance for multi-fractured horizontal wells in shale oil reservoirs.

Three regions are assumed in the proposed model: the hydraulic fracture, which is perpendicular to reservoir and regarded as infinite conductivity. And opened bedding, which is result in fracturing stimulation. As well as matrix, where contains numerous unopened beddings and shale matrix, and handle with equivalent parameters through Kazemi dual-medium model. Dynamic drainage area(DDA)concept is used to handle transient linear flow in each region.

The main influencing factors of flowback and early production have been clarified.

The proposed model, which can consider flow geometry and boundary conditions runs faster than numerical models, which provides a model foundation for achieving efficient automatic history matching.

REFERENCE

[1] Fang HH, Li A, Sang SX, Gu CC, Yang J, Li L, Liu HL, Xu HJ, Huang YH. Numerical analysis of permeability rebound and recovery evolution with THM multi-physical field models during CBM extraction in crushed soft coal with low permeability and its indicative significance to CO_2 geological sequestration. Energy 2023; 262(Part A): 125395.

[2] Sun FR, Yao YD, Chen MQ, Li XF, Zhao L, Meng Y, Sun Z, Zhang T, Feng D. Performance analysis of superheated steam injection for heavy oil recovery and modeling of wellbore heat efficiency. Energy 2017; 125:795–804.

[3] Sun FR, Yao YD, Li XF. The Heat and Mass Transfer Characteristics of Superheated Steam Coupled with Non-condensing Gases in Horizontal Wells with Multi-point Injection Technique. Energy 2018; 143:995–1005.

[4] Wen K, Qiao D, Nie C, Lu Y, Wen F, Zhang J, et al. Multi-period supply and demand balance of large-scale and complex natural gas pipeline network: economy and environment. Energy 2023;264:126104.

[5] Zhou YB, Li HS, Huang JL, Zhang RL, Wang SJ, Hong YD, Yang YL. Influence of coal deformation on the Knudsen number of gas flow in coal seams. Energy 2021; 233: 121161.

[6] Sun F. R., Yao Y. D., Li G. Z., Dong M. D. Transport behaviors of real gas mixture through nanopores of shale reservoir. J Pet Sci Eng 2019; 177: 1134-1141.

[7] Ma Y, Ardakani OH, Zhong N, Liu H, Huang H, Larter S. Possible pore structure deformation effects on the shale gas enrichment: an example from the Lower Cambrian shales of the Eastern Upper Yangtze Platform, South China. Int J Coal Geol 2020;217:103349.

[8] Guo Z, Lv X, Liu C, Liu X, Liu Y. Prediction of organic richness in shale gas reservoirs using a novel organic-inorganic decoupling seismic inversion method. Gas Sci Eng 2023; 110:204864.

[9] Male F. Using a segregated flow model to forecast production of oil, gas, and water in shale oil plays. J Pet Sci Eng 2019; 180:48-61.

[10] Clarkson CR, Williams-Kovacs J. Modeling two-phase flowback of multifractured horizontal wells completed in shale. SPE-J 2013; 18 (4):795-812.

[11] Clarkson CR, Qanbari F. A semi-analytical forecasting method for unconventional gas and light oil wells: a hybrid approach for addressing the limitations of existing empirical and analytical methods. SPE Reservoir Eval Eng 2014; 18(1):260-263.

[12] Li X, Li Q, Hu Y, Chen Q, Peng J, Xie Y, Wang J, Wu Y. Study on Three-Dimensional Dynamic Stability of Open-Pit High Slope under Blasting Vibration. Lithosphere 2021; Special 4 (2022): 6426550.

[13] Liu W, Zhang X, Fan J, Zuo J, Zhang Z, Chen J. Study on the mechanical properties of man-made salt rock samples with impurities. J Nat Gas Sci Eng 2020; 84:103683.

[14] Zhang X, Liu W, Jiang D, Qiao W, Liu E, Zhang N, Fan J. Investigation on the influences of interlayer contents on stability and usability of energy storage caverns in bedded rock salt. Energy 2021; 231:120968.

[15] Zhang SC, Guo TK, Zhou T, Zou YS, Mou SR. Fracture propagation mechanism experiment of hydraulic fracturing in natural shale. Acta Petrolei Sinica 2014; 35(3): 496-503.

[16] Xu D, Hu RL, Gao W, Xia JG. Effects of laminated structure on hydraulic fracture propagation in shale. Pe Explor Dev 2015; 42(4): 523-528.

[17] Zhou T, Wang HB, Li FX, Li YZ, Zou YS, Zhang C. Numerical simulation of hydraulic fracture propagation in laminated shale reservoirs. Pe Explor Dev 2020; 47(5): 1117-1130.

[18] Wattenbarger, R.A., El-Banbi, A.H., Villegas, M.E., & Maggard, J.B. . (1998). Production Analysis of Linear Flow Into Fractured Tight Gas Wells. *SPE Rocky Mountain Regional/Low-Permeability Reservoirs* Symposium. Society of Petroleum Engineers.

[19] Wang ZK, Cheng LS, Hamdi H, Jia P, Cao RY, Clarkson CR. A semi-analytical model for quantifying the inter-well communication in water-bearing shale gas-condensate reservoirs. Geo Sci Eng 2023; 228: 211997.
[20] Jia ZH, Cheng LS, Feng HR, Cao RY, Jia P, Pu BB, Pan QY, Shi JJ. Full composition numerical simulation of CO_2 utilization process in shale reservoir using projection-based embedded discrete fracture model (pEDFM) considering nano-confinement effect. J Nat Gas Sci Eng 2023; 111: 204932.